Transformations of citral over bifunctional Ru-H-Y-80 extrudates in a continuous reactor

Zuzana Vajglová [a], Marisa Navas [a], Päivi Mäki-Arvela [a], Kari Eränen [a], Narendra Kumar [a], Markus Peurla [b], Dmitry Yu. Murzin [a,*]

[a] Åbo Akademi University, Johan Gadolin Process Chemistry Centre, Henriksgatan 2, Turku/Åbo 20500, Finland
[b] Institute of Biomedicine, University of Turku, Kiinamyllynkatu 10, Turku 20500, Finland

ABSTRACT

One-pot transformations of citral were investigated over Ru-catalysts in a batch and a continuous mode over a powder catalyst and extrudates, respectively. Ru/H-Y-80 catalysts were prepared by different impregnation methods to obtain different particle sizes of Ru.

The highest yield of isopulegols was 15% and yield of menthols was 3% with stereoselectivity to the desired (±)-menthol isomer of 42% after 5 h over the Ru/H-Y-80 powder catalyst with the smallest metal particles prepared by the incipient wetness impregnation method with six impregnation steps using $Ru(NO)(NO_3)_3$ as a precursor. This catalyst was synthesized with the Bindzil binder and shaped by extrusion.

For comparison, also a catalyst with Ru deposited on the binder was prepared. Addition of 30 wt% Bindzil binder to Ru/H-Y-80 catalyst caused significant catalyst deactivation. Z/E-citral ratio decreased with increasing Ru particle size. Citral conversion and the yield of acyclic hydrogenation products were higher over the powder catalysts containing a mixture of zeolite and binder with a larger distance between the metal and the acid sites, i. e. with Ru deposited on the Bindzil binder. Long-term experiments in the continuous mode revealed comparable catalytic behaviour of both Ru-extrudates with the controlled metal location due to the presence of diffusion regime. The maximum yield of menthols, 6%, with stereoselectivity to the desired (±)-menthol of 73% was obtained during the transient state, below 2 h of time-on-stream. The reuse of Ru/H-Y-80 extrudates was successfully demonstrated.

1. Introduction

Menthol is a cyclic monoterpene alcohol widely used today in pharmaceutical, cosmetic and food industries, due to its flavoring properties and the cooling effect [1]. It is produced from natural sources by separation of the essential oil of *Mentha piperita or Mentha canadensis* [2], but also can be obtained *via* synthetic ways. The Takasago process utilizes myrcene as a reactant together with a homogeneous catalyst and is the most widely used [3]. The asymmetric isomerization of geranyldiethylamine in THF forming (R)-citronellal enamine catalyzed by a homogeneous chiral $[Rh((S)-BINAP)]^+$ complex is the key step in this process [4]. On the other hand, in the Haarmann & Reimer process, racemic (±)-menthols are produced *via* thymol hydrogenation being then separated by crystallization [5].

In the recent years, BASF has developed a new continuous process of L-menthol production (with at least 99.7% purity) using citral as a raw material (Fig. 1). This is a multi-staged process [6–12] involving: production of Z-citral (neral, > 97% purity) rich fraction by fractional distillation of Z/E-citral (1); selective asymmetric hydrogenation of citral to mainly the desired enantiomer D-citronellal catalyzed with a homogeneous chiral $Rh(acac)(CO)_2$/Chiraphos catalyst at 30 °C and 100 bar of H_2 (2,); cyclization of citronellal to isopulegol in the presence of an acidic catalyst bis(diarylphenoxy) aluminium at 10 °C in 5 h (3); isopulegol separation of isopulegol from the post-reaction mixture by distillation under a reduced pressure of 100 mbar and subsequent isopulegol purification by crystallization at ca. 10 °C (4); hydrogenation of L-isopulegol (>99% purity) to L-menthol at 100 °C and 50 bar in the presence of a Ni catalyst (nickel oxide) modified with Zr, Cu and Mo oxides (5); purification of L-menthol (>99.7 purity) by distillation (6).

A new alternative for the production of menthol is the synthesis from citral or citronellal using heterogeneous bifunctional catalysis. An interesting option is the one-pot synthesis from citral, which requires

three main steps: the initial hydrogenation of the conjugated C=C bond of citral to citronellal, there after cyclization of citronellal to isopulegol, and finally hydrogenation of isopulegol to menthol [13].

This approach resulting in a mixture of menthols isomers is inherently different from the BASF technology, which comprises several purification steps along with asymmetric hydrogenation. Subsequently the one-pot approach considered in this study should be completed with a separation step if a particular menthol isomer (e.g. L-menthol) is the desired product. Such separation was beyond the scope of the current work focusing exclusively on the one-pot catalytic transformations of citral.

For this purpose bifunctional catalysts are currently used, consisting of a metal supported on an acidic support. The latter promotes cyclization, while the metal catalyzes hydrogenation reactions. The choice of the support and the metal to be used is of vital importance, since they lead to the formation of various products, and therefore directly influences in selectivity. Menthol has four stereoisomeric pairs, with (-)-menthol having the characteristic cooling effect [1]. Therefore several studies reported aiming at finding an active and selective catalyst that directs the reaction towards the formation of the desired menthol isomer, avoiding also undesired side reactions. Such side reactions, are for example, citronellal hydrogenation to citronellol. Moreover, isopulegols and menthols can be defunctionalized to p-menthenes and p-menthanes. In addition, citronellal and isopulegol can form undesired dimers [14,15].

Among the supports previously used for one-pot reactions, mainly needed in the cyclization of citronellal, it is possible to mention such materials with the acidic properties as Zr-Beta, MCM-41, MCM-22, β and Y zeolites, as well as ZrOH, ZrO_2-PO_4 or ZrO_2-SO_4 [16–21]. Several studies have demonstrated that the use of zeolites containing both Lewis and Brønsted acid sites, allows to obtain the (±)-isopulegol stereoisomer as the predominant product [16,22,23]. The presence of strong acid sites is not favorable, leading otherwise to formation of the undesired by-products [20,23,24]. Plößer et al. [25] studied cyclization of citronellal, and found that a high Si:Al ratio in the zeolites used as support, increases selectivity towards menthol. However, the fraction of defunctionalized reaction products is also increased, obviously requiring more research to improve selectivity.

One-pot synthesis of menthol from citronellal, with Ru and Pt being the most active metals for this reaction has been reported. For example, Plößer et al. reached selectivity to menthol exceeding 93% at almost complete conversion of citronellal, when 1% Ru/H-BEA-25 was employed as a catalyst. The catalyst was also highly diastereoselective, producing 79% of the desired (±)-menthol [25]. Mertens et al. obtained 88% stereoselectivity and 85% yield to (–)-menthol using 2% Pt/H-beta zeolite [26]. Azkaar et al. recently studied one-pot menthol synthesis from citronellal in a trickle bed reactor, using Ru/H-beta-300 zeolite

extrudates, reaching stereoselectivity to menthol in the range of 67 to 73% [27].

Citral, which can be obtained from distillation of essential oils, is even a better alternative as a raw material, due to its renewability [28]. A simplified reaction route from citral to menthol is shown in Fig. 2, while a more complex scheme with potential side reactions and diastereoisomers was reported in [24]. Mäki-Arvela et al. studied formation of menthol from citral, employing different metals supported on H-MCM-41. The most active catalysts contained Pd and Ni as active metals [18]. Trasarti et al. also studied this synthesis in a one-step process, using various metals over zeolite Beta and Al-MCM-41 as acidic supports. The best performance was found for 3 wt% Ni/Al-MCM-41 catalyst, which yielded ca. 89% menthols and gave 72% of racemic (±)-menthol, at 100% of citral conversion after 5 h under 70 °C, 5 bar H_2, with 1 g of powder catalyst and citral/toluene ratio of 2/150 (ml) [29]. In another related work, Trasarti et al. reached higher yields (from 67 to 94%) of menthol when the Ni content was increased from 3.6 wt% to 11.4 wt%, employing SiO_2-Al_2O_3 as the support, at 100% of citral conversion after 5 h under 70 °C, 2 bar H_2, with 1 g of powder catalyst, Ni particle size of 10–14 nm and citral/toluene ratio of 2/150 (ml) [30]. This indicates that selectivity is closely related to the combination of active sites density and strength of bifunctional acid/metal sites which is needed to promote the desired pathway, avoid coke formation and subsequent catalyst deactivation.

Several studies have shown that not only the selection of the metal is important to obtain high selectivity values, but also aspects related to the synthesis of the catalysts. Plößer et al. have studied the influence of the precursor, as well as the reduction temperature in citronellal transformation to menthol over Ru/H-BEA [15]. Among the studied catalysts, the one prepared from Ru(NO)(NO₃)₃ exhibited the best activity in citronellal transformation. The catalysts prepared from this precursor also exhibited smaller metal particle sizes than those prepared from RuCl₃.

On the basis of this previous research, our work is focused on developing catalytic materials that allow to obtain menthol from citral in one step, by carrying out the selective cyclization and hydrogenation reactions towards the desired reaction products. Herein, we report preparation of bifunctional catalysts based on Ru supported on H-Y-80 zeolite, synthesized by different methods, involving incipient wetness impregnation and impregnation-evaporation methods. These catalysts were characterized and finally applied in citral transformation. The synthesis method of the best performing catalyst was scaled up and synthesized with the binder to gram amounts, characterized and tested in citral transformations in a batch reactor. This catalyst was also shaped and applied in continuous citral transformations in a trickle bed reactor to compare the effect of mass transfer limitations on catalyst activity and selectivity. The applied procedure allowed correlation of the catalyst
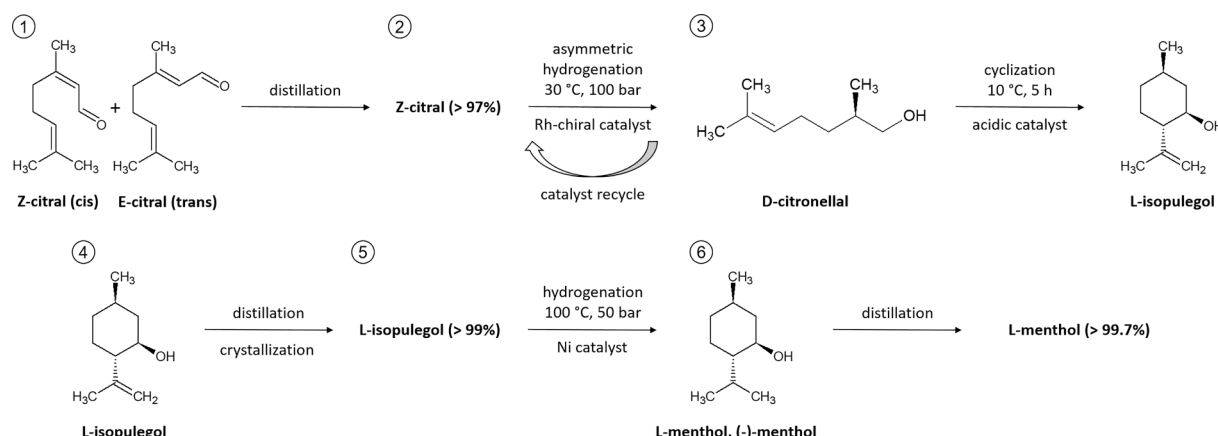

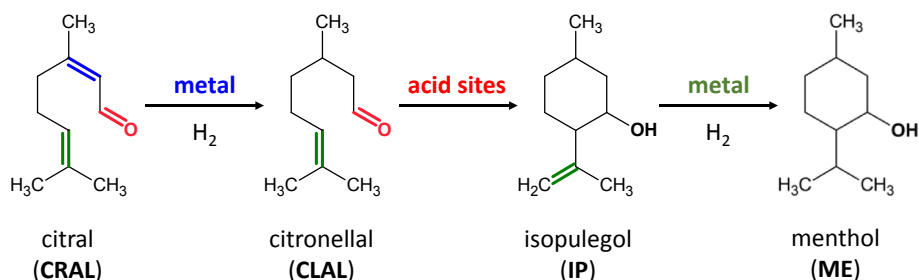**Fig. 1.** BASF's process of L-menthol production.

Fig. 2. A simplified route of citral transformation to menthol without side-reactions or diastereomers.

properties with catalytic performance.

2. Experimental

2.1. Catalyst preparation

Nine Ru-catalysts were prepared by different impregnation methods, denominated as: 1P, 2P, 3P, 4P, 4M, 4E, 5P, 5M and 5E (Table 1). The employed supports were commercial acidic H-Y-80 zeolite (SiO_2/Al_2O_3 ratio = 80, Zeolyst International), nonacidic Bindzil-50/80 (50% colloidal silica in water, Akzo Nobel) or a mixture of 70% H-Y-80 zeolite and 30% Bindzil-50/80 as a binder. Before their use, these materials were sieved to obtain particles < 63 μm. Ru was impregnated on the zeolite or the binder, depending on the case. $RuCl_3 \cdot xH_2O$ or $Ru(NO)(NO_3)_3$ (Aldrich) were employed as a Ru source. The metal nominal loading was 4.3 wt% in catalysts with zeolite as support, and 3 wt% in catalysts with the mixed support, extrudates.

Two different methods were employed to impregnate Ru over H-Y-80 zeolite: incipient wetness impregnation (IWI, [20,24]) and wet mixing including impregnation-evaporation steps (EI, [27]). The employed method for each catalyst is detailed in Table 1.

Catalyst 1P was prepared by EI method. Initially, an aqueous solution containing the precursor $Ru(NO)(NO_3)_3$ and the support H-Y-80 was stirred at 50 rpm at 60 °C during 24 h. Then, water was evaporated under vacuum at 40 °C. The obtained solid was dried at 110 °C overnight. After drying, the catalyst was calcined at 400 °C via employing two different ramps: from room temperature to 200 °C at 2.7 °C/min (holding: 50 min), and from 200 °C to 400 °C at 4.4 °C/min (holding 180 min). The R1 method was employed for the metal reduction: heating until 350 °C at 10 °C/min, and holding for 2 h under 40 mL/min H_2 flow. The reduction temperature was selected on the basis of the H_2-TPR experiment results described below.

Catalysts 2P, 3P, 4P and 5P were prepared by the Incipient wetness impregnation method (IWI) on acidic H-Y-80 zeolite (2P-4P) or nonacidic dry Bindzil (5P), introducing variations in the number of impregnation steps and the precursor used. The impregnation was carried out from an aqueous solution of $RuCl_3 \cdot xH_2O$ or the selected amount of $Ru(NO)(NO_3)_3$. The necessary volume was employed in 1 or 6 steps. In all cases, the prepared catalyst was dried at 110 °C overnight after each impregnation step. The reduction method was denoted as R2, consisting of heating to 350 °C at 2 °C/min and holding that temperature for 3 h, by 40 mL/min H_2.

Catalysts 4P and 5P were prepared in grams amount, by IWI method in 6 steps, using $Ru(NO)(NO_3)_3$ and $RuCl_3 \cdot xH_2O$ as precursor, respectively. 4P was prepared over H-Y-80 zeolite, and 5P over the Bindzil binder, in order to have the ratio 70:30 between the zeolite and Bindzil.

Catalysts 4 M and 5M correspond to Ru powder material comprising a mixture of the zeolite and the binder, prepared from 4P and 5P, over the mixed support. After impregnation, the necessary amount of the Bindzil binder or H-Y-80 zeolite was added, in order to obtain 70% zeolite and 30% binder as a support in both cases. The synthesis was performed by wet-mixing at 25 °C for 24 h under stirring at 50 rpm [20,24,27,31–33]. The shaping of the catalysts (4M and 5M) to the cylindrical bodies (4E and 5E extrudates) was carried out using a mechanical force applied in an extrusion device (TBL-2, Tianjin Tianda Beiyang Chemical Co. Ltd., China). The slurry for extrusion was prepared in the weight ratio 56.2/42.8/1.0 for the catalyst powder/distilled water/methylcellulose. The latter was used as an organic binder. The extrudates were shaped into cylinders with a diameter of 1.5 mm at ca. 10 cm/min extrusion rate driven by the continuous rotational velocity of 1400 rpm. Finally, the catalysts (4E and 5E) were dried at 100 °C, calcined, reduced employing the R1 method, and finally cut into pieces of 1 cm. During calcination at 400 °C for 3 h, methylcellulose was burnt out from the final extrudates [20,24,32,33].

2.2. Catalyst characterization

Nitrogen physisorption was performed to determine the textural properties of the H-Y-80 support, as well as fresh and spent extrudates. For that purpose, a Sorptometer Micromeritics (Micromeritics 3Flex-3500) was employed, operating at −196 °C. The samples were pretreated at 180 °C for 5 h before each measurement. The Dubinin-Radushkevich equation and the density functional theory (DFT) methods were used to determine the specific surface area, and pore volume and pore size distribution.

Transmission electron microscopy (TEM) was employed to obtain images of the catalysts and the median particle size. For that purpose, a JEM-1400 Plus equipment was employed. The catalysts were analyzed using the software ImageJ. For each sample, the median was calculated from 250 or more measurements.

Elemental analysis of the catalysts was done by inductively coupled plasma – optical emission spectrometry (ICP-OES), using PerkinElmer Optima 5300 DV.

Fourier transform infrared spectroscopy (FTIR) was employed to establish the amount of Brønsted and Lewis acidic sites present in each sample, employing an ATI Mattson FTIR Infinity Series equipment, and pyridine as a probe molecule. For each test, a pellet of 10–20 mg was prepared. The catalyst was outgassed for 2 h at 450 °C and at 0.08 mbar, and then the background signal was recorded at 100 °C. After that,

Table 1

Summary of different preparations employed. Legend: IM – impregnation method, IS – impregnation steps, RM – reduction method, EI – evaporation-impregnation method, IWI - incipient wetness impregnation method, P – powder, M – a mixture of the zeolite and the binder, E – extrudates.

Catalyst		Ru-source	IM	IS	RM
P	H-Y-80	–	–	–	–
Z	SiO_2, Bindzil binder	–	–	–	–
1P	Ru/H-Y-80	$Ru(NO)(NO_3)_3$	EI	1	R1
2P	Ru/H-Y-80	$RuCl_3 \cdot xH_2O$	IWI	6	R2
3P	Ru/H-Y-80	$RuCl_3 \cdot xH_2O$	IWI	1	R2
4P	Ru/H-Y-80	$Ru(NO)(NO_3)_3$	IWI	6	R2
4M	Ru/H-Y-80 + 30% Bindzil	–	–	–	–
4E	Ru/H-Y-80 + 30% Bindzil, E	–	–	–	–
5P	Ru/Bindzil	$RuCl_3 \cdot xH_2O$	IWI	6	R2
5M	Ru/Bindzil + 70% H-Y-80	–	–	–	–
5E	Ru/Bindzil + 70% H-Y-80, E	–	–	–	–

pyridine was adsorbed at 100 °C for 30 min. Finally, the spectra for all samples were recorded at 250 °C, 350 °C and 450 °C to measure strong, medium and weak acidic sites. The value at 250 °C is the sum of weak, medium and strong acid sites; at 350 °C, the sum of medium and strong sites; and finally, the value at 450 °C corresponds to strong acid sites. Lewis and Brønsted acidity were calculated employing the bands at 1450 cm^{-1} and 1550 cm^{-1}, respectively, applying the extinction coefficient of Emeis [34].

Temperature programmed reduction (H$_2$-TPR) was carried out using Micromeritics Auto Chem 2910. Before measurements, the non-reduced catalyst (100 mg) was dried at 100 °C overnight. The temperature program was: 25 °C −10 °C/min −120 °C (hold 60 min) with Ar flow (20 mL/min), thereafter the gas was changed to a mixture of 5 vol% H$_2$ in Ar (20 mL/min) and heated with 10 °C/min to 700 °C. The outlet gases were monitored by a thermal conductivity detector (TCD) to analyze the hydrogen consumption with respect to temperature in H$_2$-TPR. During H$_2$-TPR a cold trap composed of liquid nitrogen-2-propanol was used to trap the formed water from entering the TC detector.

Details of the physico-chemical characterization methods and equipment are presented in our previous publications [20,24,27,31–33].

2.3. Catalytic tests

Hydrogenation of citral in the batch mode was performed in a pressurized reactor (Parr Autoclave, 300 mL) under 10 bar of hydrogen (AGA, 99.999%) using cyclohexane as a solvent. The selected temperature was 70 °C and the stirring rate was 1000 rpm. The initial citral (*cis-/trans*-isomer ~1/1, ≥ 95.0%, Sigma-Aldrich) concentration was 0.086 M, and the total volume of the liquid phase was 90.2 mL. For each experiment, 100 mg of catalyst were employed. Before each reaction, the catalyst was reduced with the corresponding reduction method (Table 1). The reaction was started when the selected temperature and pressure were reached, employing an extra heated vessel to inject the citral, diluted in a part of the solvent.

The same temperature, pressure, solvent, and the initial citral concentration were used also in the continuous mode. Namely, extrudates (10 × 1.5 mm, 0.7 g) were mixed with 15 g of inert quartz of the size 0.2–0.8 mm and loaded into a trickle-bed reactor operating in a co-current downflow mode (I.D. 1.25 cm, [20,24,27,32,33]). Extrudates were reduced *in-situ* with the same reduction procedure as described above. The liquid residence time was 12.5 min at 0.4 mL/min of the feed and 50 mL/min of hydrogen. A trickling flow regime in the trickle-bed reactor was confirmed by analysis of flow map considering low gas and liquid flow rates [20,35,36].

The liquid samples were taken at different reaction times, and then diluted with cyclohexane, in order to be analyzed by gas chromatography. For that purpose, an Agilent GC 6890 N gas chromatograph, equipped with a capillary column DB-1 (30 m × 250 µm × 0.5 µm) and a FID detector, was employed. A temperature program was set, starting at 110 °C, followed by a ramp rate of 0.4 °C/min to 130 °C, and then with a ramp rate of 13 °C/min to 200 °C. The temperature of the FID detector was 340 °C. Helium was used as a carrier gas. The products were confirmed with Agilent GC/MS 6890 N/5973 using the same temperature program and the column.

Definitions are presented in the Supporting Information (SI).

3. Results and discussion

3.1. Characterization results of Ru-catalyst

H$_2$-TPR experiment with catalyst 4P (Ru/H-Y-80 from Ru(NO) (NO$_3$)$_3$) (Fig. S1) revealed complete reduction at 275 °C (T$_R$) with a maximum rate at 201 °C (T$_{Rmax}$). This is in line with the literature [37] dealing with unsupported ruthenium (oxide) from RuCl$_3$ hydrate (T$_R$ = 267 °C, T$_{Rmax}$ = 202 °C). For Ru/H-Y-80 powder catalyst containing 30 wt% of the Bindzil binder (4M), a lower reduction temperature (T$_R$ =

201 °C, T$_{Rmax}$ = 173 °C, Fig. S1) was observed.

Table 2 summarizes the characterization data of the supports and Ru-catalysts. TEM analysis confirmed that different impregnation procedures led to a different particle size of ruthenium (1.5–12 nm; Figs. S2, S3). Dispersion of Ru (11–89%, Table 2) was calculated using the formula described by Sholten et al. [38] (SI, eq. 1) assuming spherical shapes of Ru, giving D$_{Ru}$ = 133/d$_{Ru}$ [39]. TEM images also show particle agglomerations on the surfaces, in particular for the catalyst 1P, in which the metal particles had a larger size. Moreover, it is possible to observe the structure of the zeolite network. The largest metal particles, ca. 12 nm, were obtained for the catalyst 1P prepared by the evaporation-impregnation method (EI) using RuCl$_3$·xH$_2$O as a precursor. On the contrary, the smallest metal particles, 1.5 nm, were observed for the catalyst 4P prepared by the Incipient wetness impregnation method (IWI) using Ru(NO)(NO$_3$)$_3$ as a precursor. Furthermore, for the catalyst 4P it is possible to distinguish Ru particles inside the zeolite channels. Comparison of the catalysts 2P and 4P, prepared with the same impregnation method (IWI involving 6 impregnation steps) but with different precursors, revealed a 3.6-fold smaller particle size on the catalyst 4P using Ru(NO)(NO$_3$)$_3$ precursor compared to RuCl$_3$·xH$_2$O. This is in line with the literature [15] dealing with Ru/H-BEA catalyst prepared using different Ru-precursors (Ru(NO)(NO$_3$)$_3$), Ru(acac)$_3$, RuCl$_3$ and Ru$_3$(CO)$_{12}$) and the reduction temperatures (250–650 °C).

Simultaneously, different impregnation procedures led also to a different Ru content (1.2–3.9 wt% of Ru on H-Y-80 zeolite, Table 2). In all cases, the real concentration was significantly lower than the nominal loading. This is attributed to the low pH value of Ru-precursors solutions, 0.3 and 1.6 for Ru(NO)(NO$_3$)$_3$ and RuCl$_3$·xH$_2$O, respectively. Namely, at a low pH of the precursor, it can be assumed that the support surface is positively charged (isoelectric point for SiO$_2$ [40,41] and zeolites [40,41] are 1.8–6.3 and 3.6–7.5, respectively) which led to repulsive interactions with the Ru^{3+} cation. In the case of zeolite Y, the zeta potential value and respective isoelectric point were not observed at pH < 3.0 because a rapid dissolution of the crystals takes place [42], at pH > 3.0 the zeta potential value was around −30 mV.

The acidity of supports and catalysts determined by pyridine adsorption-desorption with FTIR is presented in detail in Table S1. After introducing Ru on H-Y-80 zeolite, the amount of weak acid sites increased>6 times, while the amount of medium and the strong acid sites decreased to 0–2 µmol/g in all cases. For catalyst 3P prepared by the IWI method with one impregnation step using RuCl$_3$·xH$_2$O precursor, significantly lower Lewis acidity (ca. 1.8–2.5 fold), and consequently a higher B/L ratio, was observed compared to other Ru/H-Y-80 catalysts. In the case of the non-acidic silica Bindzil binder (5P), the amount of weak Brønsted acid sites significantly increased, from zero to 10 µmol/g, after Ru impregnation. The concentration of weak Lewis acid sites increased only slightly, from 1 to 2 µmol/g. This led to a high B/L ratio of 6.2. This is consistent with the literature [20,24,43–45] which states that the metal introduction (Ru, Pt) on the catalyst always leads to a significant decrease in the strong Brønsted and the strong Lewis acid sites, and subsequently to a change in weak and medium acidity depending on the type of the support material. On the contrary to Ru introduction on SiO$_2$ (5P), after 2 wt% Pt introduction on SiO$_2$, only the concentration of weak Lewis acid sites increased from 0 to 9 µmol/g [43].

Overall, different real concentrations of Ru and acidity of the catalysts led to a wide range of the metal-to-acid site ratio (c$_{Ru}$/c$_{AS}$ = 0.3–9.8, Table 2). In the case of Ru/H-Y-80 catalysts, the metal-to-acid site ratio increased with decreasing the size of Ru.

Analysis of textural properties (Table 2, Fig. 3) showed a high specific surface area (823 m^2/g) and the pore volume (0.47 cm^3/g) of pristine H-Y-80 microporous zeolite, containing 62% of the micropore volume with a median pore diameter of 0.78 nm. On the contrary, a pristine mesoporous Bindzil binder exhibited a relatively low specific surface area (157 m^2/g), containing 97% of mesopore volume with a median pore diameter of 2.9 nm. After the metal introduction, the

Table 2

Characterization data of the support and Ru-catalysts. In parenthesis data for the spent catalyst. Legend: c_{Ru} – Ru concentration in the entire volume; d_{Ru} – Ru particle size; D_{Ru} – metal dispersion ($133/d_{Ru}$) [38,39]; TAS – total acid sites; BAS – Brønsted acid sites; LAS – Lewis acid sites; B/L – ratio of Brønsted and Lewis acid sites; c_{AS} – concentration of total acid sites; A – specific surface area; V_p – specific pore volume; $V_{\mu p}$ – micropore volume.

| Cat.	c_{Ru} %	d_{Ru} nm	D_{Ru} %	TAS μmol/g	BAS μmol/g	LAS μmol/g	B/L -	c_{Ru}/c_{AS} -	A m^2/g	V_p cm^3/g	V_μ cm^3/g
P	–	–	–	39	24	15	1.6	–	823	0.47	0.29
Z	–	–	–	2	1	1	1.0	–	157	0.30	0.01
1P	2.0	11.9 (11.9)	11	30	18	11	1.7	0.7	–	–	–
2P	1.2	5.4 (5.6)	25	37	23	15	1.6	0.8	–	–	–
3P	2.8	2.8 (2.6)	48	27	20	6	3.1	4.9	–	–	–
4P	3.9	1.5 (1.5)	89	35	20	15	1.3	9.8	575	0.32	0.21
4M	1.0	6.7 (6.8)	20	23	14	9	1.5	0.8	413	0.29	0.15
4E	0.8	9.4 (8.7)	14	26	16	10	1.6	0.4	409 (156)	0.30 (0.18)	0.15 (0.06)
5P	4.0	6.5 (6.8)	21	12	10	2	6.2	6.7	33	0.13	0.00
5M	0.6	8.2 (7.9)	16	21	11	10	1.1	0.5	423	0.27	0.15
5E	0.6	7.2 (8.9)	19	33	18	15	1.2	0.3	398 (192)	0.26 (0.18)	0.14 (0.07)
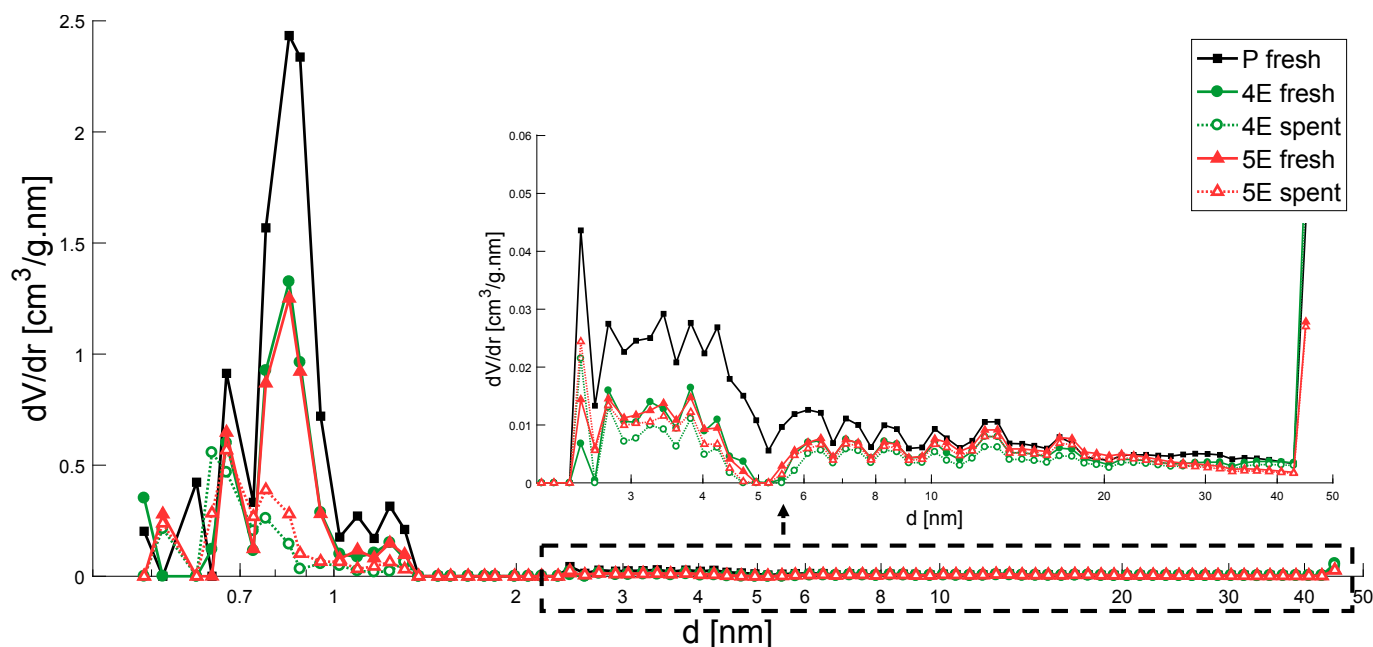
Fig. 3. Pore size distribution of the fresh and the spent catalysts. Legend: fresh powder H-Y-80 zeolite without the metal (P fresh, black square), fresh (Ru/H-Y-80) + Bindzil extrudates (4E fresh, green circle), spent (Ru/H-Y-80) + Bindzil extrudates (4E spent, open green circle), fresh (Ru/Bindzil) + H-Y-80 extrudates (5E fresh, red triangle), spent (Ru/Bindzil) + H-Y-80 extrudates (5E spent, open red triangle). (For interpretation of the references to colour in this figure legend, the reader is referred to the web version of this article.)

specific surface area and the pore volume decreased by ca. 30% and by ca. 70% in the case of Ru/ H-Y-80 (4P) and Ru/Bindzil (5P) catalysts, respectively. The final surface area of Ru/H-Y-80 catalyst (4P, 575 m²/ g) was 17.4 fold higher than for Ru/Bindzil (5P, 33 m²/g). A similar reduction of the specific surface area (by 34%) after impregnation was observed for Pt/H-Beta-25 with bentonite [44]. After mixing of catalysts 4P, 5P with the necessary amount of the Bindzil binder or H-Y-80 zeolite, in order to obtain 70% zeolite and 30% binder as a support in both cases, the textural properties, including the pore size distribution were comparable (Table 2, Fig. 3). In both cases, only a slight decrease in the specific surface area was observed for the final extrudates 4E, 5E compared to the powder form of catalysts 4M, 5M. The pore volume and pore size distribution were not affected by the mechanical force during extrusion (Table 2, Fig. 3).

Overall, in the case of powder catalysts containing a mixture of the zeolite and the binder 4M, 5M and their respective extrudates 4E, 5E with the same composition but different Ru deposition, textural properties, acidity, and the metal particle size were similar. A slightly lower Ru concentration and B/L ratio were observed for the catalysts with Ru located on the Bindzil binder compared to the catalysts with Ru located

on the H-Y-80 zeolite. A slightly lower specific surface area, and a slightly higher acidity for extrudates than for the powder catalysts is attributed to the process of shaping and calcination of extrudates [32,33,46,47], during which the micropore mouths became partially blocked and extraframework alumina was formed, respectively. The pristine H-Y-80 zeolite is characterized by hexagonal particles and other particles with sharp edges of the size of 0.5–1 μm (determined by SEM, [48]), while the Bindzil binder particles are significantly smaller being of a spherical shape with a broad size range of 0.02–0.29 μm (determined by SEM, [49]). Based on the previous results of SEM analysis of extrudates containing 70% of the catalyst and 30% binder [20,33,44,45], it can be assumed that for Ru-extrudates containing 70% H-Y-80 zeolite and 30% Bindzil binder, used in the current work and prepared by the same procedure, the binder was also distributed homogeneously in the shaped body. However, locally, the chemical interfacial interactions were observed [20,33,44,45].

The mechanical resistance of extrudates used in the current work was sufficient for a stable catalytic performance in the trickle-bed reactor. Generally, the mechanical strength of extrudates containing a catalyst (Beta-25, ZSM-5) and 20–30 wt% of the silica binder is ca. 0.2–3.5 MPa

(metal-free extrudates, [32,50]) and ca. 2.9–4.5 MPa (Pt extrudates, [45]) in a vertical position.

After the reaction, only negligible changes in the metal particle size were observed for all catalysts (Table 2, Figs. S2, S3) confirming absence of sintering. On the contrary, the specific surface area and the micropore volume of extrudates decreased by>50% (Table 2, Fig. 3), which could be related to coke formation [18,20,24]. Pore blockage was observed mainly in the pores with a diameter of 0.7–1 nm (Fig. 3).

3.2. Activity and selectivity of powder Ru-catalysts in the batch experiments

Fig. 3 displaying citral concentrations and Z/E-citral ratio as a function of Ru particle sizes at the same normalized time (ca. $8.5 \cdot 10^{-6}$ h·mol$_{Ru(surface)}$) clearly shows a slower transformation of citral over catalysts with Ru deposited on the Bindzil binder (5P, 5M, red triangles). In the case of the catalysts with Ru deposited on the H-Y-80 zeolite (1P-4P, 4M), the maximum of Z-citral concentration was observed at ca. 4 nm, i.e. the slowest transformation is expected over the catalyst exhibiting Ru cluster size between 2.8 and 5.4 nm. E-citral transformation slowed down with increasing Ru particle sizes up to 5.4 nm, thereafter remaining constant. Z/E-citral ratio decreased linearly with increasing Ru particle size, and the lower values were observed for the catalyst with Ru located on the H-Y-80 zeolite (Fig. 4d). Contrary to [24] reporting Ru/H-MCM-41 catalysts with 30 wt% of Bindzil, in the current work citral hydrogenation is seen to be dependent on the particle size of ruthenium. The sensitivity of Z-citral compared to non-sensitivity of E-citral could be tentatively attributed to different adsorption modes and requires further studies.

Comparison with extrudates at 12.5 min of residence time showed the same trend as for the powder catalyst (1P-4P, 4M, Fig. 4) only for the reused catalyst with Ru deposited on H-Y-80, after 24 h time-on-stream (4E II). Extrudates 4E and 5E at 12 h of TOS exhibited a lower concentration of citral and a slightly lower value of Z/E-citral ratio than the powder catalyst at a similar Ru particle size.

Fig. 5 displays concentration profiles of citral as a function of normalized time (SI), taking into account the catalyst mass, concentration, and the Ru dispersion (SI). For all powder Ru/H-Y-80 catalysts with different particle sizes of Ru tested in the batch experiments, the concentration profiles were comparable. Furthermore, in line with the literature [18,24], Z-citral (neral) was transformed always faster than E-citral (geranial) over Ru/H-Y-80 catalysts. Z/E-citral ratio decreased with the reaction time faster over Ru/H-Y-80 catalysts with a larger Ru particle size (Fig. 5d). An exception is Ru/SiO$_2$ catalyst (5P), exhibiting deactivation transformation rate was approximately the same for both citral isomers. The primary data of citral concentration profile are reported in the Supporting Information (Fig. S4).

Catalytic data (Fig. 6) shows that, in the beginning of the experiment, citral conversion was almost independent on the ruthenium particle size and on the support (Fig. 6b). Thereafter, significant differences were observed for catalysts with different supports. Conversion over Ru/H-Y-80 (3P, 4P) was up to two-fold higher than over Ru/SiO$_2$ (5P) at the same normalized time of $4.5 \cdot 10^{-5}$ h·mol$_{Ru(surface)}$. This may be related to the low specific surface area and porosity of the catalyst 5P and its deactivation because of coking.

The liquid phase mass balance closure and carbon balance (MB, CB, Fig. 5c) were similar for all powder catalysts being ca. 80%. Slightly higher MB and CB, ca. 90% were obtained for the catalyst 2P. In citral and citronellal transformations to menthol over Ru/H-MCM-41 catalysts containing 30 wt% of Bindzil, the same MB was also observed, ca. 80% [20,24]. Similar MB values (77–100%) were reported for citronellal transformations to menthol over the powder Ru and Pt/H-Beta-25 catalysts containing 30 wt% of Bentonite [27]. At the same normalized time of $8.5 \cdot 10^{-6}$ h mol$_{Ru(surface)}$, the total yield (Fig. 6d) was the lowest for the less acidic catalyst 5P (Y = 5.3%), and the highest for the catalyst 2P (Y = 19.1%) with the highest acidity and the median particle size of Ru (d_{Ru} = 5.4 nm, Table 2 among the studied catalysts). The maximum total yield (Y = 39.2%) and citral conversion (X = 59%) were obtained after 5 h at $1.7 \cdot 10^{-4}$ h mol$_{Ru(surface)}$ of normalized time using the catalyst 4P with the highest Ru content, the smallest Ru particle size and the lowest B/L ratio.

Although the catalytic activity was similar for the Ru/H-Y-80 catalysts with different particle sizes of Ru, significant differences were observed in term of selectivity in citral transformation in the batch reactor (Fig. 7). For all Ru/H-Y-80 catalysts, hydrogenation activity was stopped while cyclic products were still increasing with time. A significantly higher yield of acyclic hydrogenation products (Y_{ACP} = 16%) was obtained using the catalyst 4P with the smallest Ru particle size (d_{Ru} =
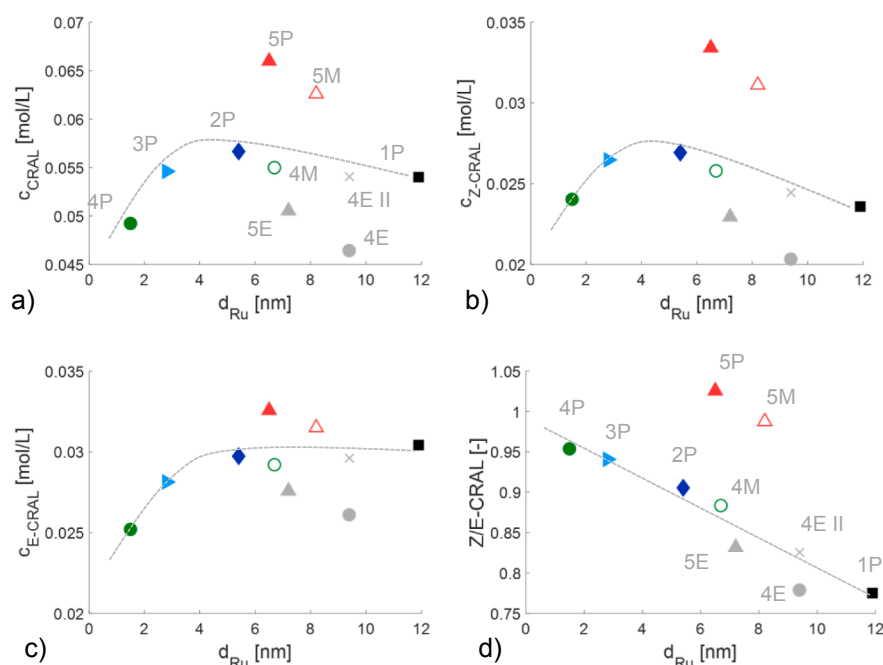

Fig. 4. Concentration as a function of Ru particle sizes at ca. $8.5 \cdot 10^{-6}$ h mol$_{Ru(surface)}$ of normalized time for the powder catalysts ($4.9 \cdot 10^{-6}$ h mol$_{Ru(surface)}$ for the catalyst 5M) and at 12 h of time-on-stream, 12.5 min of residence time for extrudates: a) racemic mixture of citral, b) Z-citral, c) E-citral; d) ration of Z-citral to E-citral. Legend: Ru/H-Y-80 (1P, black square), Ru/H-Y-80 (2P, dark blue diamond), Ru/H-Y-80 (3P, light blue triangle), Ru/H-Y-80 (4P, green circle), Ru/Bindzil (5P, red triangle), Ru/H-Y-80 + Bindzil (4M, open green circle), Ru/Bindzil + H-Y-80 (5M, open red triangle), Ru/H-Y-80 + Bindzil extrudates (4E, grey circle), reused Ru/H-Y-80 + Bindzil extrudates (4E (II) reused, grey cross), Ru/Bindzil + H-Y-80 extrudates (5E, grey triangle). Conditions: 70 °C, 10 bar of H$_2$, 0.086 M initial concentration of citral in cyclohexane, 0.1 g of the powder catalyst, 0.7 g of extrudates. (For interpretation of the references to colour in this figure legend, the reader is referred to the web version of this article.)
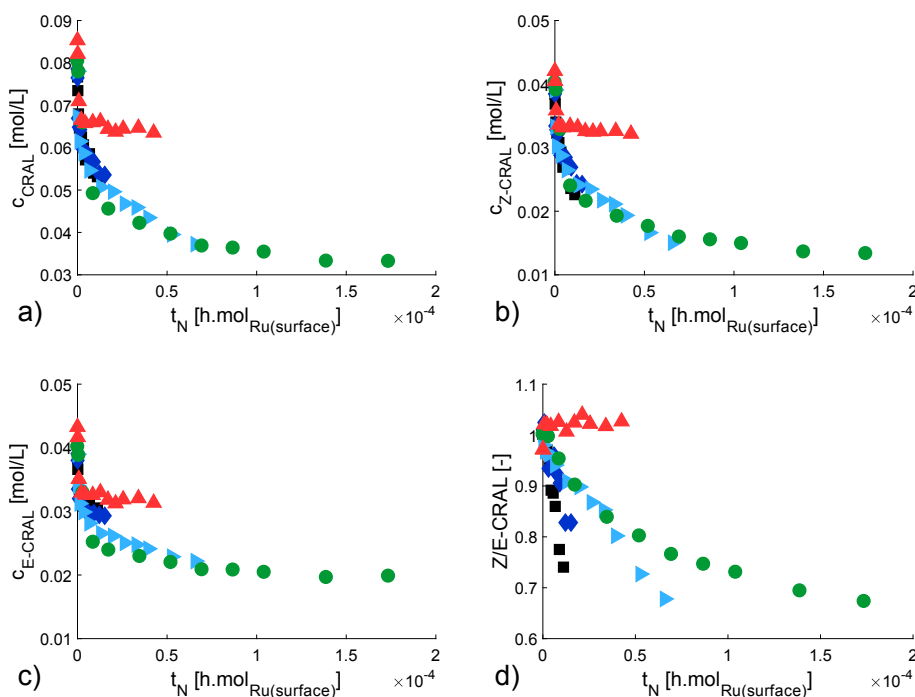
Fig. 5. Concentration profiles as a function of normalized time: a) racemic mixture of citral, b) Z-citral, c) E-citral; d) ratio of Z-citral to E-citral as a function of normalized time. Legend: Ru/H-Y-80 (1P, black square), Ru/H-Y-80 (2P, dark blue diamond), Ru/H-Y-80 (3P, light blue triangle), Ru/H-Y-80 (4P, green circle), Ru/Bindzil (3P, red triangle). Conditions: batch experiment, 70 °C, 10 bar of H_2, 0.086 M initial concentration of citral in cyclohexane, 0.1 g of catalyst. (For interpretation of the references to colour in this figure legend, the reader is referred to the web version of this article.)
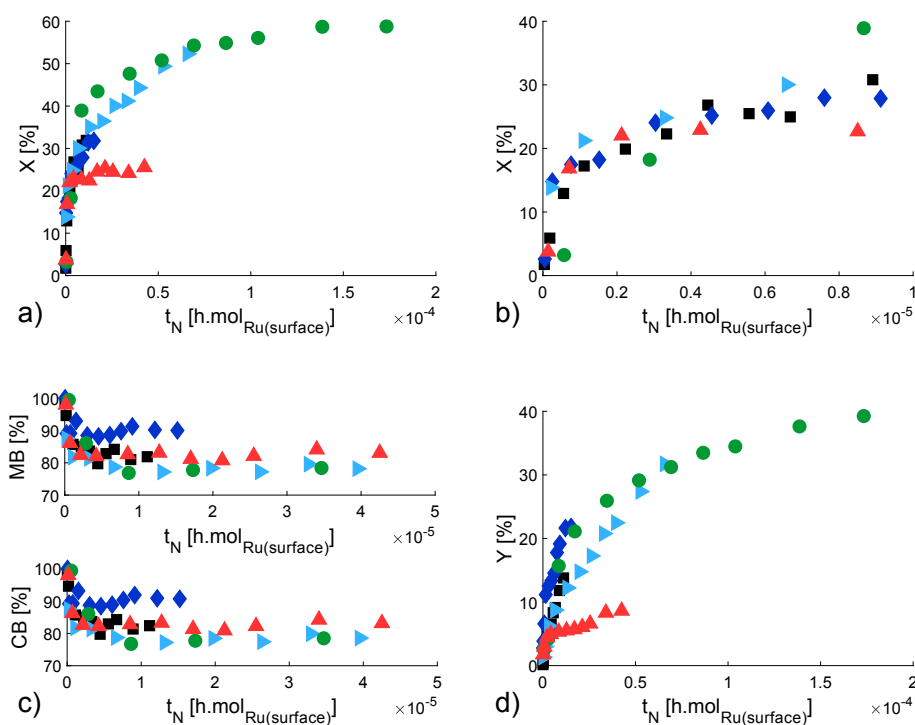
Fig. 6. Citral transformations over Ru powder catalyst in the batch reactor: a,b) conversion of citral, c) liquid phase mass balance closure (MB) and carbon balance (CB), d) total yield as a function of normalized time. Legend: Ru/H-Y-80 (1P, black square), Ru/H-Y-80 (2P, dark blue diamond), Ru/H-Y-80 (3P, light blue triangle), Ru/H-Y-80 (4P, green circle), Ru/Bindzil (3P, red triangle). Conditions: 70 °C, 10 bar of H_2, 0.086 M initial concentration of citral in cyclohexane, 0.1 g of catalyst. (For interpretation of the references to colour in this figure legend, the reader is referred to the web version of this article.)

1.5, Table 2) compared to other materials. The obtained maximum yield of acyclic hydrogenation products was correlated with the particle size of ruthenium (Ru dispersion), regardless of the catalyst support (Fig. S5a,b).

At the beginning of the reaction, the main product was composed of acyclic hydrogenation products, especially citronellal (S_{CLAL} = 40–100%), and later, isopulegols (S_{IPs} = 36–45%). This is opposite to some previous studies [20,24], where mainly defunctionalization products were formed, namely p-menthatrienes in citronellal and citral transformation. It is attributed to the ca. 2-fold higher acidity of Ru/H-

MCM-41 catalysts with the Bindzil binder [20,24]. Different behaviour was observed with Ru/SiO$_2$ (5P), i.e. hydrogenation activity was increasing with increasing time while cyclic products ceased to be formed. The product mixture at citral conversion of 26%, contained 80% of ACP (citronellal 60%, 2,6-dimethyloctane 9%, geraniol 6%, nerol 3%, citronellol 3%), 7% of isopulegols, and 13% of defunctionalization products. Contrary, 17% of isopulegols, and 83% of ACP, mainly geraniol + nerol (56%) along with citronellal (27%), were obtained over 0.75% Ru/SiO$_2$ powder at citral conversion of 5% after 2.8 h at 27 °C and atmospheric pressure [51].
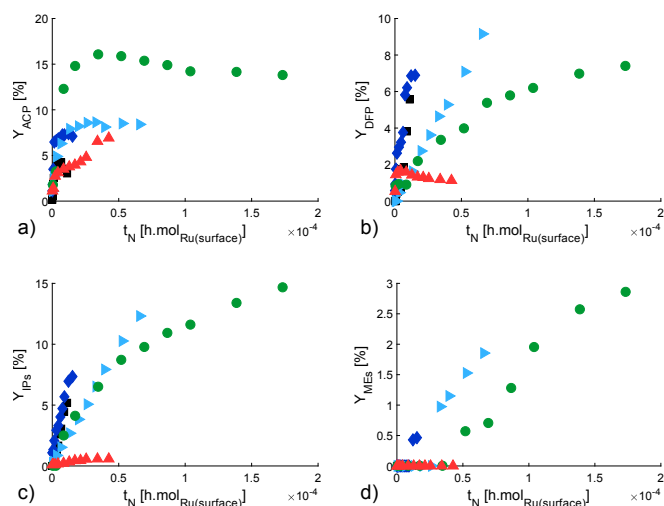
Fig. 7. Product distribution in citral transformations over Ru powder catalyst in the batch reactor: a) yield of acyclic hydrogenation products, b) yield of defunctionalization products, c) yield of isopulegols, d) yield of menthols as a function of normalized time. Legend: Ru/H-Y-80 (1P, black square), Ru/H-Y-80 (2P, dark blue diamond), Ru/H-Y-80 (3P, light blue triangle), Ru/H-Y-80 (4P, green circle), Ru/Bindzil (3P, red triangle). Conditions: 70 °C, 10 bar of H_2, 0.086 M initial concentration of citral in cyclohexane, 0.1 g of catalyst. (For interpretation of the references to colour in this figure legend, the reader is referred to the web version of this article.)

Overall, selectivity to defunctionalization products (DFP) and isopulegols (IPs) increased with decreasing selectivity to acyclic hydrogenation products (Figs. S5c,d). Comparison of the results at the same normalized time of $8.5 \cdot 10^{-6}$h $mol_{Ru(surface)}$, shows that selectivity of ACP and CP increased and decreased, respectively, with increasing metal-to-acid site ratio (c_{Ru}/c_{AS}) (Figs. S6a,b). Moreover, the DFP/IPs ratio decreased from 1.1 to 0.36 with increasing c_{Ru}/c_{AS} from 0.7 to 9.8 in the case of Ru/H-Y-80 catalysts (1P-4P), i.e. formation of isopulegols was preferred over the catalyst with a higher c_{Ru}/c_{AS} ratio. An exception is Ru/SiO2 catalyst (5P), where the ca. 15-fold higher value of the DFP/

IPs ratio was obtained (Fig. S6c). This could be related to a significantly higher B/L ratio compared to other catalysts (Figs. S6d) and generally to a very low Lewis acidity (2 µmol/g, Table 2).

The highest yield of isopulegols (Y_{IPs} = 14.7%) was obtained after 5 h for the catalyst 4P with the lowest B/L ratio and the smallest particle size of Ru. Overall, it is known that stereoselectivity to isopulegol isomers in citronellal or citral transformations can strongly depend on the catalyst, namely on acidity [14,21,22,25,26,32,33,52] and the metal location [20,24]. Most of heterogeneous catalysts, such as H-ZSM-5 [22,25], Zr (OH)4 [16], ZrO2-SO2 [25], Al2O3-SiO2 [25], H3PMo12O40 [25], H3PW12O40 [25], H-MCM-41 [22], Ru/H-Beta-300 [27], Pt, Ru/H-Beta-25 + Bentonite [27], Ru/H-MCM-41 + Bindzil [20,24], do not allow to surpass the thermodynamic equilibrium ratio of (±)-isopulegol/diastereoisomers, 75:25. In citronellal transformations, stereoselectivity to (±)-isopulegol adhering close to the thermodynamic equilibrium (71–75%), has been reported for H-ZSM-10 [52], Beta zeolites [22,52], Pt/H-Beta [22], SiO2 [22]. A significantly higher stereoselectivity to (±)-isopulegol (90–94%) was obtained with Lewis acids catalysts ZnBr2, ZnCl2, Zr-Beta [21,25,52], and Sc(OTf)3 [53] also in citronellal transformation.

In the current work, different distribution of the four isopulegol diastereomers (Fig. 8) was obtained over Ru supported on the same H-Y-80 zeolite (1P-4P) but with a different particle size of Ru. It should be also noted that the stereoisomers ratio was changed during the reaction, especially for the catalyst with a larger Ru particle size (1P, 2P). It was explained either by different rates of isopulegol hydrogenation to menthols or interconversion between different isopulegols [20]. At the same normalized time of $8.5 \cdot 10^{-6}$h $mol_{Ru(surface)}$, the isopulegol stereoselectivity was in the range: (35–65)/(26–38)/(0–20)/(0–39) of IP/NI/IIP/NIIP (Table S2). In the case of 5P catalyst (Ru/SiO2), only IIP isomer was obtained with a very low yield of 0.6%, which can be attributed to extremely low Lewis acidity (2 µmol/g, Table 2).

Stereoselectivity to the desired (±)-isopulegol was clearly correlated with the yield of citronellal (Y_{CLAL}) and the ratio of the Brønsted to Lewis acid sites (B/L) as Y_{CLAL}/(B/L) (Fig. S7a). In other words, the amount of (±)-isopulegol increased when more citronellal was formed. The latter increases with Ru dispersion, and, at the same time, with a decreasing B/L ratio, i.e. with higher Lewis acidity.
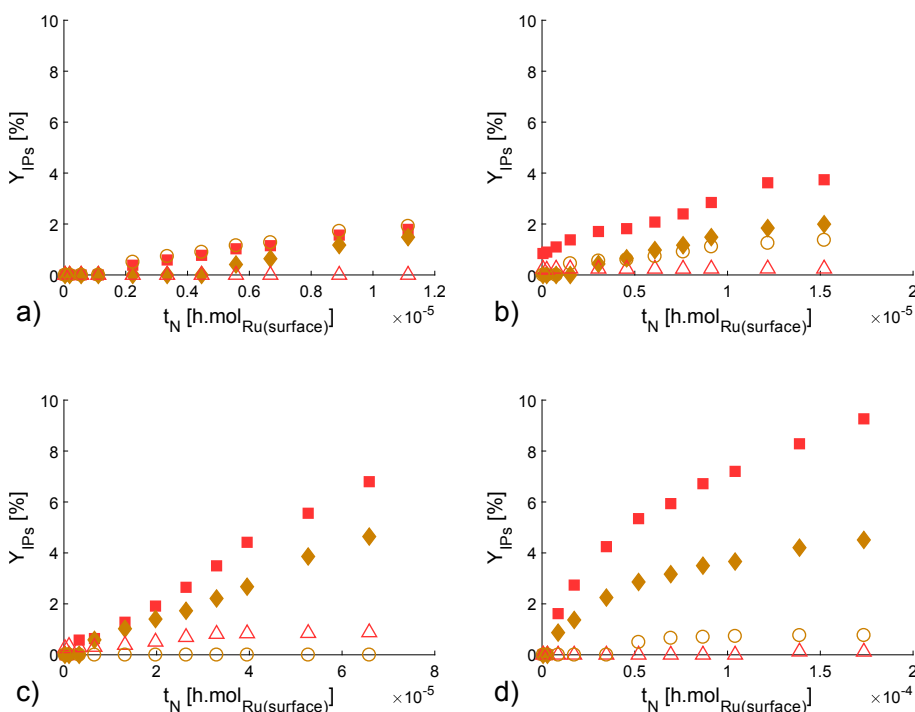

Fig. 8. The yield of isopulegol isomers as a function of normalized time in citral transformations over Ru/(H-MCM-41 + Bindzil-50/80) powder catalyst in the batch reactor: a) Ru/H-Y-80 (1P), b) Ru/H-Y-80 (2P), c) Ru/H-Y-80 (3P), d) Ru/H-Y-80 (4P). Conditions: 70 °C, 10 bar of H_2, 0.086 M initial concentration of citral in cyclohexane, 0.2 g of catalyst. Legend: isopulegol (red, filled square), neoisopulegol (orange, filled diamond), isoisopulegol (red, empty triangle), neoisoisopulegol (orange, empty circle). (For interpretation of the references to colour in this figure legend, the reader is referred to the web version of this article.)

The yield of menthols increased with increasing yield of isopulegols (Fig. S7c), i.e. the highest yield of menthols (Y_{MEs} = 2.9%) was obtained after 5 h over the catalyst 4P with the smallest particle size of Ru and subsequently with the highest Ru dispersion. Distribution of the four menthol diastereomers changed depending on the particle size of Ru (Fig. 9). No menthols were detected for the 1P catalyst with the largest Ru particle size (11.9 nm, Table 2). Only isomenthol (IME) was observed for 2P with the Ru particle size of 5.4 nm. Isomenthol (IME) and neo-isomenthol (NIME) with the ratio of 54 to 46% were obtained over the 3P catalyst with Ru particle size of 2.8 nm. Only with 4P exhibiting the smallest Ru particle size of 1.5 nm, the desired menthol was detected with stereoselectivity of 42%, followed by 35% and 23% to IME and NIME, respectively. In this case, the lower stereoselectivity to (±)-menthol isomer could be attributed to the overall low yield of all menthol isomers (Y_{MEs} = 2.9%) at mediocre transformation of citral (X = 59%). This is linked to the lower yield of isopulegols obtained in the previous step, which also increases with conversion (Fig. S7a) and to a relatively high amount of the acyclic hydrogenation products formed at the first 15 min of the reaction (S_{ACP} = 79%). On the contrary, in the synthesis of menthol from citronellal [25] over 0.5 g of Ru/H-Beta catalysts with different Ru particle sizes (1–11 nm) and Ru concentration (1–4 wt%) at 100 °C, 25 bar and 4.5 g citronellal, 150 mL *n*-hexane and 1 mL *n*-tetradecane, diastereoselectivity to the desired menthol was comparable (SS_{ME} = 67–73%) over all catalysts at citronellal conversion of 91–100% after 40 min [25]. Only structure-sensitivity of defunctionalization was reported in [25] similar to the data generated in the current work (Fig. 7). Lower stereoselectivity to the menthol isomer of 47%, followed by 37% and 16% to IME and NME, respectively, was only obtained from citral using 1 g of 1 % Pd/Beta catalyst which was explained by a high value of the rate constant of citronellal to 3,7-dimethyloctanal on Pd [29]. No menthol isomers were also detected with the Ru/SiO$_2$ catalyst (5P) with the medium Ru particle size (6.5 nm). This result is related to an extremely low yield of isopulegols obtained in the previous step.

A significantly higher yield of menthols (ca. 89%, [21]) with stereoselectivity to the desired menthol of ca. 72% obtained from citral over 3 wt% Ni/Al-MCM-41 catalyst at 100% of citral conversion after 5 h under 70 °C, 5 bar H$_2$, with 1 g of the powder catalyst and the citral/

toluene ratio of 2/150 (ml) could be also related to a lower electronegativity of Ni (1.91) compared to Ru, Pd or Pt (2.2 or 2.28, respectively).

3.3. Activity and selectivity of Ru- powder catalysts containing a mixture of a zeolite and a binder in the batch experiments

Ru/H-Y-80 catalyst (4P) with the smallest particle size of Ru achieving the highest yield of menthols was synthesized with the Bindzil binder (as the powder catalyst 4M) and then shaped into cylindrical extrudates (4E). For comparison also the Ru/Bindzil catalyst (5P) was synthesized with H-Y-80 zeolite (as 5M) and later shaped (5E). Both catalysts (powder 4M, 5M and extrudates 4E, 5E) with different Ru location were tested in batch and trickle-bed reactors.

Comparison of the citral concentration profile (Fig. S8) revealed that adding H-Y-80 zeolite to Ru/Bindzil catalyst led to negligible changes while 30 wt% Bindzil binder together with 70% Ru/H-Y-80 catalyst resulted in significant deterioration of catalytic activity. The citral conversion, obtained after 5 h, decreased by ca. 50%, i.e. from 59% (4P) to 29% (4M). At the same time, the Z/E-citral ratio was also significantly changed in the case of the catalyst (4M) where Ru was deposited on the zeolite. It can be related to ca. 4.5-fold increased Ru particle size for 4M compared to 4P. That is supported by a comparison with the Ru/H-Y-80 catalyst 2P (Fig. S8) having a similar Ru particle size (5.4 nm, Fig. S2, Table 2) with Ru/H-Y-80 + Bindzil catalyst 4M (6.7 nm, Fig. S3, Table 2) even if acidity was slightly higher for the 2P catalyst.

Although the total acidity and Lewis acidity were the same, and the Ru particle size and textural properties were comparable for both powder catalysts with controlled metal location (4M, 5M), the citral conversion, and the yield of acyclic hydrogenation products were higher over the catalyst 5M with a larger distance between the metal to acid sites (Figs. S9 and S10). This observation is in line with the literature [24] reporting Ru/H-MCM-41 catalyst with the Bindzil binder. On the contrary, the yield of cyclic products such as isopulegols and defunctionalization products was higher for the catalyst 4M with a short distance between metal to acid sites (Figs. S10 and S11). However, the stereoselectivity to (±)-isopulegol was slightly higher for the catalyst 5M (Fig. S11). Menthols were not detected over any of the catalysts 4M, 5M.
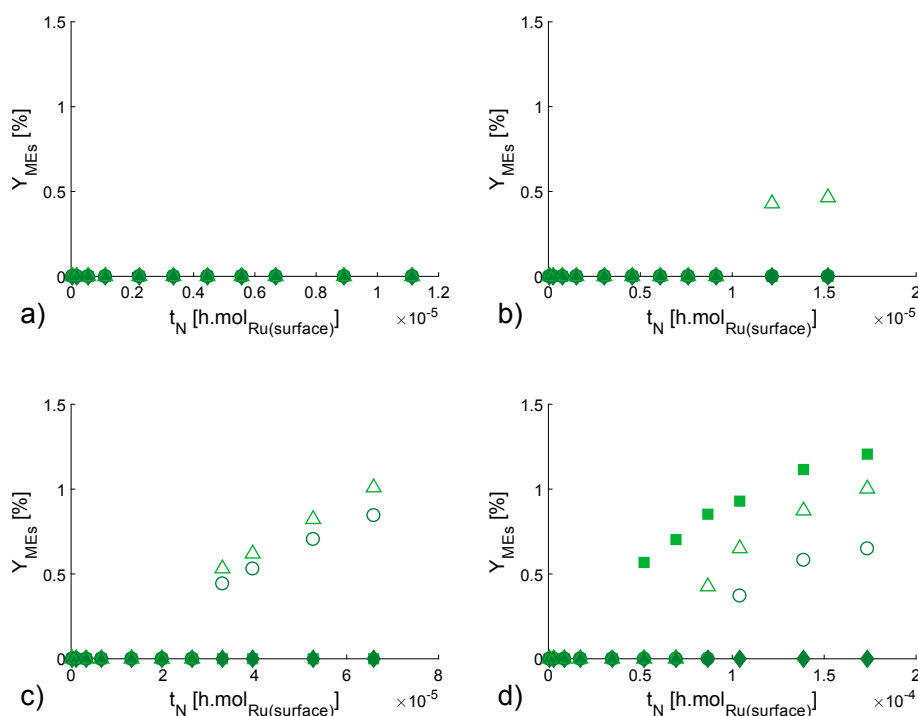

Fig. 9. The yield of menthol isomers as a function of normalized time in citral transformations over Ru/(H-MCM-41 + Bindzil-50/80) powder catalyst in the batch reactor: a) Ru/H-Y-80 (1P), b) Ru/H-Y-80 (2P), c) Ru/H-Y-80 (3P), d) Ru/H-Y-80 (4P). Conditions: 70 °C, 10 bar of H$_2$, 0.086 M initial concentration of citral in cyclohexane, 0.2 g of catalyst. Legend: menthol (light green, filled square), neomenthol (dark green, filled diamond), isomenthol (light green, empty triangle), neoisomenthol (dark green, empty circle). (For interpretation of the references to colour in this figure legend, the reader is referred to the web version of this article.)

The same as for Ru-catalysts (1P-5P) described above, also for Ru-powder catalysts containing a mixture of the zeolite and the binder (4M, 5M) the maximum yield of the acyclic hydrogenation products (ACP) decreased with increasing Ru dispersion (Fig. S5a,b), and selectivity to ACP decreased with decreasing the metal-to-acid site ratio (Fig. S6a,b).

3.4. Activity and selectivity of Ru-extrudates in the continuous experiments

As in [24] were Ru/H-MCM-41 catalysts with the Bindzil binder were reported, also in the current work, the experiments in the trickle-bed reactor under trickling flow regime [20,35,36] showed comparable catalytic behaviour for both Ru/H-Y-80 + Bindzil extrudates with the controlled metal location (4E, 5E) (Fig. 10), i.e. for extrudates location of Ru was of minor importance, which can be explained by significant influence of mass transfer. The presence of the regime with diffusional limitations was confirmed by comparing the cumulative reaction rates and turnover frequency over powder and shaped Ru-catalysts (Table S3). The effectiveness factor for extrudates (4E, 5E) vs the powder catalysts containing a mixture of the zeolite and the binder (4M,5M) was calculated to be 0.11–0.13 (Table S3, $\eta = r_E/r_M$). This is ca. 2-fold lower than for Ru/H-MCM-41 extrudates with the Bindzil binder having ca. 2-fold lower value of porosity [24].

Long-term experiments (12 h) in the continuous mode revealed the transient behaviour in the first 3–4 h of time-on-stream (TOS), characterizing dynamics of the processes in the reactor. During this time, the citral conversion decreased to ca. 25%, the liquid phase mass balance closure (MB), respectively carbon balance (CB), increased to ca. 95%, and the total yield reached a maximum at 2 h of TOS (ca. 35%) subsequently decreasing to ca. 20–25%. The lower MB, CB (50–80%) observed after 3 h in citronellal transformations to menthol over Ru and Pt/H-Beta-25 extrudates containing 30 wt% of the Bentonite binder was attributed previously to formation of some heavy compounds, not visible in GC analysis [27].

The observed maximum of the total yield during the transient stage, along with the maxima in the yields of the acyclic hydrogenation, and defunctionalization products, and also menthols, could be attributed to the coke formation [18,20,24], i.e. blocking of the active sites followed a decrease of catalytic activity (Fig. 10).

A comparison with Ru-powder catalysts containing a mixture of the zeolite and the binder in the batch experiments showed that Ru-extrudates at the steady-state, i.e. after 12 h of TOS with residence time of 12.5 min, achieved a slightly lower citral conversion and selectivity to ACP (Table S3). On the contrary, a slightly higher total yield, and selectivity to isopulegol and menthols were detected (Table S3, Fig. 11).

After 12 h of TOS, the stereoselectivity to (±)-isopulegol was 25% for both extrudates (4E, 5E) (Fig. 12, Table S3). This is 1.6–1.8 fold lower

than for the Ru-powder catalysts containing a mixture of the zeolite and the binder (4M, 5M) at a similar conversion (Table S3). The obtained stereoselectivity to (±)-isopulegol over Ru-extrudates is in line with the correlation reported above (Fig. S7).

Overall, selectivity to the intermediate products is lower for the internal mass transfer regime, thus selectivity to the final product is higher [54]. Menthols (Fig. 13) were obtained only over extrudates (4E, 5E), but not with Ru-powder catalysts containing a mixture of the zeolite and the binder (4M, 5M). The maximum total yields of the menthols isomers achieved were 6% and 5.8% with the stereoselectivity to the desired (±)-menthol of 73% and 72% at 1 h and 2 h of TOS, respectively, for the extrudates 4E and 5E, respectively. For the extrudates 5E with Ru located on the Bindzil binder, the yield of menthols decreased to zero after 12 h of TOS. For the extrudates 4E with Ru located on H-Y-80, the yield of menthols decreased to 0.7% with menthol to isomenthol ratio of 49:51. A similar result was obtained also for the reused catalyst 4E II after 12 h of TOS, i.e. $Y_{MEs} = 0.6\%$, ME:IME = 47:53 (Table S2).

The catalyst 4E was consecutively reused (4E II) to elucidate catalyst deactivation. Regeneration was carried out by simply washing the catalyst with cyclohexane solvent (for 30 min under 0.5 mL/min). In comparison to the fresh catalyst, the transient stage was obtained without a decreased conversion of citral and without any maxima of the yields. In the steady-state, negligible changes were observed in terms of citral conversion, the liquid phase mass balance closure, yield, and also product distribution. Generally, the results obtained over the reused extrudates (4E II) were comparable with the results over the fresh extrudates 4E obtained at the steady-state, i.e. after 4 h of TOS. These results showed clearly reusability of Ru-based extrudates regenerated by simple washing with the solvent.

A comparison of the result obtained at similar conditions in the trickle-bed reactor over Ru extrudates (10 × 1.5 mm) with different acidic supports is summarized into Table S4. Acidity of the selected catalysts (total/Brønsted/Lewis acid sites) was as follows: 207/159/48 μmol/g for Ru/H-Beta-25 + bentonite [27] > 52/29/22 μmol/g for Ru/H-MCM-41 + bindzil [24] > 26/16/10 μmol/g for Ru/H-Y-80 + bindzil. All extrudates had Ru deposited exclusively on the catalytic material with comparable Ru particle sizes of 9.4–10 nm. The specific surface area was in the range of 409–520 m^2/g and Ru concentration was the lowest one (0.8 wt%) for the least acidic Ru/H-Y-80 extrudates and the highest one (3.2 wt%) for the most acidic Ru/H-Beta-25 extrudates at the same nominal loading of 2 wt%. A comparison clearly showed that lower acidity increased formation of the acyclic hydrogenation product. This led to formation of a higher amount of isopulegols and subsequently a higher amount of menthols even at lower conversion levels when citral was used as a starting material. Simultaneously, the yield of defunctionalization products was ca. 2-fold lower and stereoselectivity to the menthol isomer was slightly higher for less acidic extrudates. On the contrary, a better result in terms of the menthols yield but with the same stereoselectivity to the desired menthol isomer was obtained when
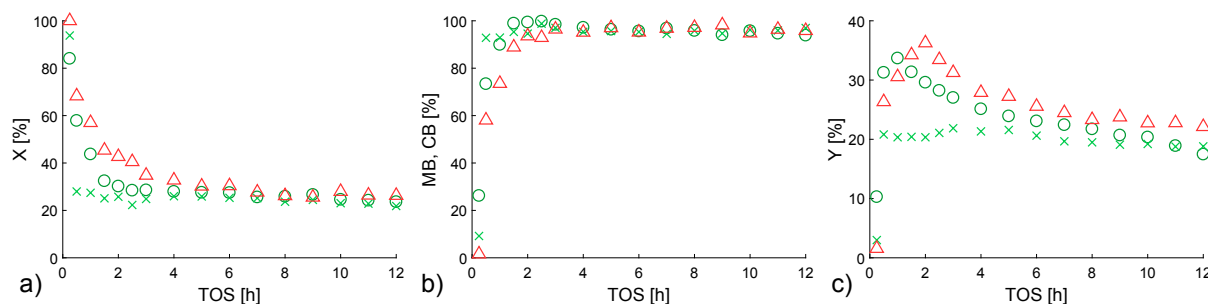

Fig. 10. Citral transformation over Ru-extrudates in the trickle-bed reactor: a) conversion of citral, b) liquid phase mass balance closure (MB) and carbon balance (CB), c) total yield as a function of time-on-stream. Legend: (Ru/H-Y-80) + Bindzil (4E, green circle), (Ru/H-Y-80) + Bindzil (4E reused, green cross), (Ru/Bindzil) + H-Y-80 (5E, red triangle). Conditions: 70 °C, 10 bar of H$_2$, 0.086 M initial concentration of citral in cyclohexane, 0.7 g of catalyst, 12.5 min of residence time. (For interpretation of the references to colour in this figure legend, the reader is referred to the web version of this article.)
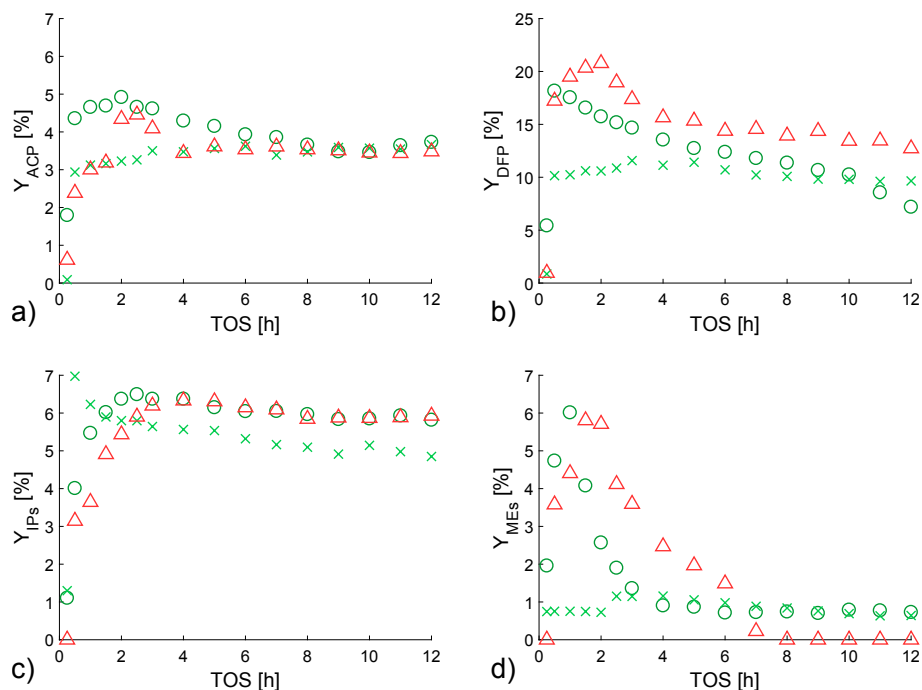
Fig. 11. Product distribution in citral transformation over Ru-extrudates in the trickle-bed reactor: a) yield of acyclic hydrogenation products, b) yield of defunctionalization products, c) yield of isopulegols, d) yield of menthols as a function of time-on-stream. Legend: (Ru/H-Y-80) + Bindzil (4E, green circle), (Ru/H-Y-80) + Bindzil (4E reused, green cross), (Ru/Bindzil) + H-Y-80 (5E, red triangle). Conditions: 70 °C, 10 bar of H_2, 0.086 M initial concentration of citral in cyclohexane, 0.7 g of catalyst, 12.5 min of residence time. (For interpretation of the references to colour in this figure legend, the reader is referred to the web version of this article.)
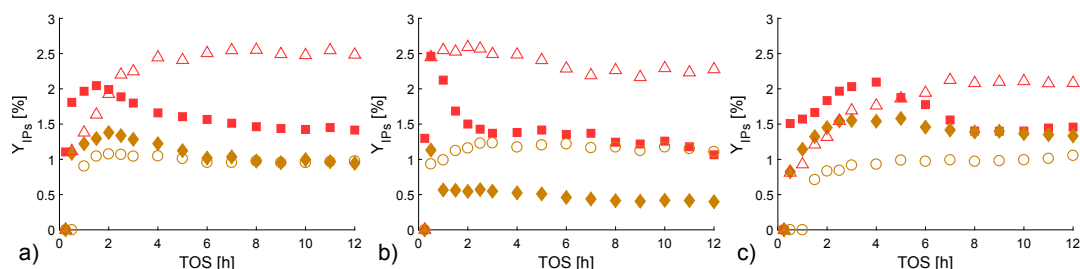

Fig. 12. The yield of isopulegol isomers as a function of time-on-stream in citral transformation over Ru-extrudates in the trickle-bed reactor: a) (Ru/H-Y-80) + Bindzil (4E, green circle), b) (Ru/H-Y-80) + Bindzil (4E reused, green cross), c) (Ru/Bindzil) + H-Y-80 (5E, red triangle). Conditions: 70 °C, 10 bar of H_2, 0.086 M initial concentration of citral in cyclohexane, 0.7 g of catalyst, 12.5 min of residence time. Legend: isopulegol (red, filled square), neoisopulegol (orange, filled diamond), isoisopulegol (red, empty triangle), neoisoisopulegol (orange, empty circle). (For interpretation of the references to colour in this figure legend, the reader is referred to the web version of this article.)
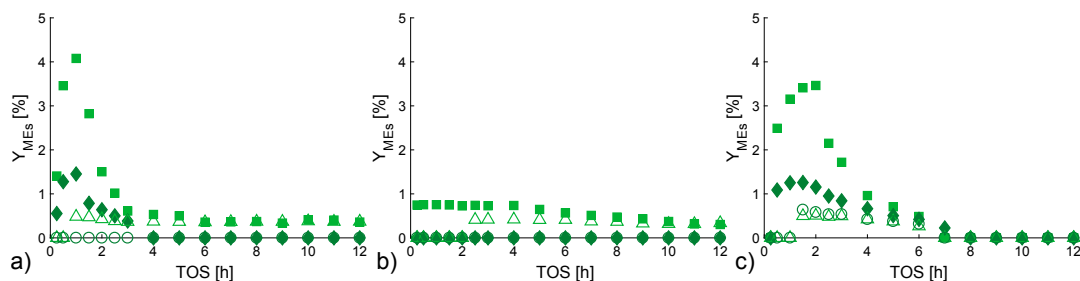

Fig. 13. The yield of menthol isomers as a function of time-on-stream in citral transformation over Ru-extrudates in the trickle-bed reactor: a) (Ru/H-Y-80) + Bindzil (4E, green circle), b) (Ru/H-Y-80) + Bindzil (4E reused, green cross), c) (Ru/Bindzil) + H-Y-80 (5E, red triangle). Conditions: 70 °C, 10 bar of H_2, 0.086 M initial concentration of citral in cyclohexane, 0.7 g of catalyst, 12.5 min of residence time. Legend: menthol (light green, filled square), neomenthol (dark green, filled diamond), isomenthol (light green, empty triangle), neoisomenthol (dark green, empty circle). (For interpretation of the references to colour in this figure legend, the reader is referred to the web version of this article.)

citronellal was used as a starting material even if acidity of Ru/H-Beta-25 + bentonite [27] was ca. 8-fold higher than for catalytic system Ru/H-Y-80 + bindzil.

4. Conclusions

One-pot transformations of citral to menthol were investigated over bifunctional Ru-catalysts in a batch and a continuous mode over powder catalysts and extrudates, respectively. Ru-catalysts were prepared by

different impregnation methods leading to different Ru particle sizes. H-Y-80 zeolite and Bindzil-50/80 were used as an acidic catalytic material and an inorganic binder, respectively. $RuCl_3 \cdot xH_2O$ or $Ru(NO)(NO_3)_3$ was used as a Ru precursor. The metal nominal loading was 4.3% in catalysts with zeolite as a support, and 3 wt% in powder catalysts with the mixed support, extrudates.

Different impregnation procedures led to different Ru particle sizes ranging between 1.5 and 12 nm, different Ru content of 1.2–3.9 wt%, and a wide range of the metal-to-acid site molar ratio of 0.3–9.8. The smallest metal particles, and simultaneously, the highest Ru content were observed for the catalyst prepared by the incipient wetness impregnation method with six impregnation steps using $Ru(NO)(NO_3)_3$ as a precursor. After the reaction, only negligible changes in the metal particle size were observed for all catalysts. On the contrary, the specific surface area and the micro-pore volume of extrudates decreased by>50%, which was attributed to coke formation, mainly in the pores with a diameter of 0.7–1 nm.

Batch experiments revealed that Z/E-citral ratio decreased linearly with increasing Ru particle size. Although catalytic activity was similar for Ru/H-Y-80 catalysts with different particle sizes of Ru, significant differences were observed in selectivity. The maximum yield of acyclic hydrogenation products was obtained with the smallest Ru particles, regardless of the catalyst support. Over Ru-catalysts supported on the same H-Y-80 zeolite but bearing a different particle size of Ru, different distributions of the four isopulegol diastereomers were obtained. Stereoselectivity to the desired (±)-isopulegol increased with an increasing yield of citronellal originating from Ru dispersion, and at the same time, with a decreasing Brønsted-to-Lewis acid site ratio. This correlation was valid for all catalysts, including the powder catalysts comprising the zeolite and the binder, and extrudates. Distribution of four menthol diastereomers changed with the particle size of Ru. Only over the catalyst with the smallest Ru particle size, the desired menthol was detected with stereoselectivity of 42%, followed by 35% and 23% to isomenthol and neoisomenthol, respectively.

Significant deterioration of the catalytic activity was observed when 30 wt% Bindzil binder was added to Ru/H-Y-80 catalyst. Citral conversion, and the yield of acyclic hydrogenation products were higher over the powder catalysts comprising the zeolite and the binder with a larger distance between the metal to acid sites, i.e. with Ru deposited on the Bindzil binder.

Long-term experiments in the continuous mode revealed comparable catalytic behaviour of both Ru-extrudates due to the impact of mass transfer counterbalancing different metal location. Selectivity to the intermediate products is lower for regime of internal mass transfer, thus selectivity to the final product is higher. The maximum yield of menthols, 6%, with stereoselectivity to the desired (±)-menthol of 73% was obtained in the transient regime, up to 2 h of time-on-stream. Extrudates washed with the solvent after the reaction showed results comparable to the fresh extrudates.

Declaration of Competing Interest

The authors declare that they have no known competing financial interests or personal relationships that could have appeared to influence the work reported in this paper.

Acknowledgments

Appendix A. Supplementary data

Definitions, catalyst characterization data and catalytic testing data. Supplementary data to this article can be found online at https://doi.org/10.1016/j.cej.2021.132190.

References

[1] T. Patel, Y. Ishiuji, G. Yosipovitch, Menthol: a refreshing look at this ancient compound, J. Am. Acad. Dermatol. 57 (2007) 873–878, https://doi.org/10.1016/j.jaad.2007.04.008.

[2] G.P.P. Kamatou, I. Vermaak, A.M. Viljoen, B.M. Lawrence, Menthol: a simple monoterpene with remarkable biological properties, Phytochemistry 96 (2013) 15–25, https://doi.org/10.1016/j.phytochem.2013.08.005.

[3] S. Otsuka, K. Tani, S. Yamagata, S. Akutagawa, H. Kumobayashi, M. Yagi, EP Patent 68506, in: Takasago (Ed.), 1972.

[4] R. Noyori, Asymmetric catalysis: science and opportunities (Nobel lecture 2001), Adv. Synth. Catal. 345 (2003) 15–32, https://doi.org/10.1002/adsc.200390002.

[5] J. Fleischer, K. Bauer, R. Hopp, DE 2109456, in: H. Reimer (Ed.), 1971.

[6] B. Lau, The Cool Freshness of Mentho, BASF SE, https://www.basf.com/us/en/media/science-around-us/the-cool-freshness-of-menthol.html (accessed 7 July 2021).

[7] J.B. Brazier, Challenges in catalysis for pharmaceuticals and fine chemicals III, Platin. Met. Rev. 56 (2012) 99–103.

[8] R. Rachawalik, Technology of monoterpenoid fragrances, Cracow University of Technology, Cracow, 2018.

[9] J.C. Leffingwell, (-)-Menthol from Geraniol or Nerol or Geranial or Neral. A New BASF Process, Leffingwell & Associates, http://www.leffingwell.com/menthol13/menthol_basf.htm (accessed 7 July 2021).

[10] J. Leffingwell, D. Leffingwell, Chiral Chemistry in Flavours & Fragrances, Flavours & Fragrances, http://www.leffingwell.com/Chem_Spec_Mag.pdf (accessed 7 July 2021).

[11] J. Gleason-Allured, BASF To Unveil New Production Site; Revamps L-Menthol Process, Perfumer & Florist, https://www.perfumerflavorist.com/flavor/rawmaterials/synthetic/160880375.html (accessed 7 July 2021).

[12] Ch.S. Sell, Fundamentals of fragrance chemistry, Wiley-VCH, Germany, 2019.

[13] C. Milone, C. Gangemi, G. Neri, A. Pistone, S. Galvagno, Selective one step synthesis of (-)-menthol from (+)citronellal on Ru supported on modified SiO_2, Appl. Catal. A-Gen. 199 (2000) 239–244, https://doi.org/10.1016/S0926-860X(99)00560-8.

[14] J. Plößer, M. Lucas, J. Wärnå, T. Salmi, D.Y. Murzin, P. Claus, Kinetics of the one-pot transformation of citronellal to menthols on Ru/H-BEA catalysts, Org. Process. Res. Dev. 20 (2016) 1647–1653, https://doi.org/10.1021/acs.oprd.6b00214.

[15] J. Plößer, F. Dedeaga, M. Lucas, P. Claus, The effect of catalyst preparation conditions on the synthesis of menthol from citronellal on Ru/H-BEA, Appl. Catal. A-Gen. 516 (2016) 100–108, https://doi.org/10.1016/j.apcata.2016.02.014.

[16] G.K. Chuah, S.H. Liu, L.J. Harrison, Cyclisation of citronellal to isopulegol catalysed by hydrous zirconia and other solid acids, J. Catal. 200 (2001) 352–359, https://doi.org/10.1006/jcat.2001.3208.

[17] C.B. Cortes, V.T. Galvan, S.S. Pedro, T.V. Garcia, One pot synthesis of menthol from (+/-)-citronellal on nickel sulfated zirconia catalysts, Catal. Today. 172 (2011) 21–26, https://doi.org/10.1016/j.cattod.2011.05.005.

[18] P. Mäki-Arvela, N. Kumar, D. Kubicka, A. Nasir, T. Heikkila, V.P. Lehto, R. Sjöholm, T. Salmi, D.Y. Murzin, One-pot citral transformation to menthol over bifunctional micro- and mesoporous metal modified catalysts: effect of catalyst support and metal, J. Mol. Catal. A-Chem. 240 (2005) 72–81, https://doi.org/10.1016/j.molcata.2005.06.023.

[19] Y.T. Nie, W. Niah, S. Jaenicke, G.K. Chuah, A tandem cyclization and hydrogenation of (+/-)-citronellal to menthol over bifunctional Ni/Zr-beta and mixed Zr-beta and Ni/MCM-41, J. Catal. 248 (2007) 1–10, https://doi.org/10.1016/j.jcat.2007.02.018.

[20] Z. Vajglová, N. Kumar, M. Peurla, K. Eränen, P. Mäki-Arvela, D.Y. Murzin, Cascade transformations of (±)-citronellal to menthol over extruded Ru-MCM-41 catalysts in a continuous reactor, Catal. Sci. Technol. 10 (2020) 8108–8119, https://doi.org/10.1039/D0CY01251C.

[21] Y.Z. Zhu, Y.T. Nie, S. Jaenicke, G.K. Chuah, Cyclisation of citronellal over zirconium zeolite beta - a highly diastereoselective catalyst to (+/-)-isopulegol, J. Catal. 229 (2005) 404–413, https://doi.org/10.1016/j.jcat.2004.11.015.

[22] P. Mäki-Arvela, N. Kumar, V. Nieminen, R. Sjöholm, T. Salmi, D.Y. Murzin, Cyclization of citronellal over zeolites and mesoporous materials for production of isopulegol, J. Catal. 225 (2004) 155–169, https://doi.org/10.1016/j.jcat.2004.03.043.

[23] A.F. Trasarti, A.J. Marchi, C.R. Apesteguia, Design of catalyst systems for the one-pot synthesis of menthols from citral, J. Catal. 247 (2007) 155–165, https://doi.org/10.1016/j.jcat.2007.01.016.

[24] Z. Vajglová, P. Mäki-Arvela, K. Eränen, N. Kumar, M. Peurla, D.Y. Murzin, Catalytic transformations of citral in a continuous flow over bifunctional Ru-MCM-41 extrudates, Catal. Sci. Technol. 11 (2021) 2873–2884, https://doi.org/10.1039/D1CY00066G.

[25] J. Plößer, M. Lucas, P. Claus, Highly selective menthol synthesis by one-pot transformation of citronellal using Ru/H-BEA catalysts, J. Catal. 320 (2014) 189–197, https://doi.org/10.1016/j.jcat.2014.10.007.

[26] P. Mertens, F. Verpoort, A.N. Parvulescu, D. De Vos, Pt/H-beta zeolites as productive bifunctional catalysts for the one-step citronellal-to-menthol

conversion, J. Catal. 243 (2006) 7–13, https://doi.org/10.1016/j.jcat.2006.06.017.

[27] M. Azkaar, P. Mäki-Arvela, Z. Vajglová, V. Fedorov, N. Kumar, L. Hupa, J. Hemming, M. Peurla, A. Aho, D.Y. Murzin, Synthesis of menthol from citronellal over supported Ru- and Pt-catalysts in continuous flow, React. Chem. Eng. 4 (2019) 2156–2169, https://doi.org/10.1039/C9RE00346K.

[28] A. Negoi, K. Teinz, E. Kemnitz, S. Wuttke, V.I. Parvulescu, S.M. Coman, Bifunctional nanoscopic catalysts for the one-pot synthesis of (+/-)-menthol from citral, Top. Catal. 55 (2012) 680–687, https://doi.org/10.1007/s11244-012-9850-y.

[29] A.F. Trasarti, A.J. Marchi, C.R. Apesteguia, Highly selective synthesis of menthols from citral in a one-step process, J. Catal. 224 (2004) 484–488, https://doi.org/10.1016/j.jcat.2004.03.016.

[30] A.F. Trasarti, A.J. Marchi, C.R. Apesteguia, Synthesis of menthols from citral on Ni/SiO2-Al2O3 catalysts, Catal. Commun. 32 (2013) 62–66, https://doi.org/10.1016/j.catcom.2012.11.030.

[31] Z. Vajglová, N. Kumar, M. Peurla, J. Peltonen, I. Heinmaa, D.Y. Murzin, Synthesis and physicochemical characterization of beta zeolite-bentonite composite materials for shaped catalysts, Catal. Sci. Technol. 8 (2018) 6150–6162, https://doi.org/10.1039/C8CY01951G.

[32] Z. Vajglová, N. Kumar, P. Mäki-Arvela, K. Eränen, M. Peurla, L. Hupa, D.Y. Murzin, Effect of binders on the physicochemical and catalytic properties of extrudate-shaped beta zeolite catalysts for cyclization of citronellal, Org. Process. Res. Dev. 23 (2019) 2456–2463, https://doi.org/10.1021/acs.oprd.9b00346.

[33] Z. Vajglová, N. Kumar, P. Mäki-Arvela, K. Eränen, M. Peurla, L. Hupa, M. Nurmi, M. Toivakka, D.Yu. Murzin, Synthesis and physicochemical characterization of shaped catalysts of beta and Y zeolites for cyclization of citronellal, Ind. Eng. Chem. Res. 58 (2019) 18084–18096, https://doi.org/10.1021/acs.iecr.9b02829.

[34] C.A. Emeis, Determination of integrated molar extinction coefficients for infrared-adsorption bands of pyridine adsorbed on solid acid catalysts, J. Catal. 141 (1993) 347–354, https://doi.org/10.1006/jcat.1993.1145.

[35] G. Mary, A. Esmaeili, J. Chaouki, Simulation of the selective hydrogenation of C-3-cut in the liquid phase, Int. J. Chem. React. Eng. 14 (2016) 859–874, https://doi.org/10.1515/ijcre-2015-0095.

[36] M.I. Urseanu, J.G. Boelhouwer, H.J.M. Bosman, J.C. Schroijen, G. Kwant, Estimation of trickle-to-pulse flow regime transition and pressure drop in high-pressure trickle bed reactors with organic liquids, Chem. Eng. J. 111 (2005) 5–11, https://doi.org/10.1016/j.cej.2005.04.015.

[37] P.G.J. Koopman, A.P.G. Kieboom, H. Vanbekkum, Characterization of ruthenium catalysts as studied by temperature programmed reduction, J. Catal. 69 (1981) 172–179, https://doi.org/10.1016/0021-9517(81)90139-1.

[38] J.J.F. Scholten, A.P. Pijpers, A.M.L. Hustings, Surface characterization of supported and nonsupported hydrogenation catalysts, Catal. Rev. Sci. Eng. 27 (1985) 151–206, https://doi.org/10.1080/01614948509342359.

[39] A.J. Plop, H. Vuori, A.O.I. Krause, K.P. de Jong, J.H. Bitter, Particle size effects for carbon nanofiber supported platinum and ruthenium catalysts for the selective hydrogenation of cinnamaldehyde, Appl. Cata. A-Gen. 351 (2008) 9–15, https://doi.org/10.1016/j.apcata.2008.08.018.

[40] X. Liu, P. Mäki-Arvela, A. Aho, Z. Vajglová, V.M. Gun'ko, I. Heinmaa, N. Kumar, K. Eranen, T. Salmi, D.Yu. Murzin, Zeta potential of Beta zeolites: Influence of structure, acidity, pH, temperature and concentration, Molecules 23 (2018) 946, https://doi.org/10.3390/molecules23040946.

[41] M. Kosmulski, pH-dependent surface charging and points of zero charge. IV. update and new approach, J. Colloid Interface Sci. 337 (2009) 439–448, https://doi.org/10.1016/j.cis.2019.102064.

[42] T. Kuzniatsova, Y. Kim, K. Shqua, P.K. Dutta, H. Verweij, Zeta potential measurements of zeolite Y: application in homogeneous deposition of particle coatings, Micropor. Mesopor. Mat. 103 (2007) 102–107, https://doi.org/10.1016/j.micromeso.2007.01.042.

[43] D. Kubička, N. Kumar, T. Venalainen, H. Karhu, I. Kubičkova, H. Osterholm, D.Y. Murzin, Metal-support interactions in zeolite-supported noble metals: influence of metal crystallites on the support acidity, J. Phys. Chem. B. 110 (2006) 4937–4946, https://doi.org/10.1021/jp055754k.

[44] Z. Vajglová, N. Kumar, M. Peurla, L. Hupa, K. Semikin, D.A. Sladkoyskiy, D.Y. Murzin, Effect of the preparation of Pt-modified zeolite beta-bentonite extrudates on their catalytic behavior in n-hexane hydroisomerization, Ind. Eng. Chem. Res. 58 (2019) 10875–10885, https://doi.org/10.1021/acs.iecr.9b01931.

[45] Z. Vajglová, N. Kumar, M. Peurla, L. Hupa, K. Semikin, D.A. Sladkovskiy, D.Y. Murzin, Deactivation and regeneration of Pt-modified zeolite beta-bindzil extrudates in n-hexane hydroisomerization, J. Chem. Technol. Biotechnol. 96 (2021) 1–11, https://doi.org/10.1002/jctb.6685.

[46] A. de Lucas, P. Sanchez, A. Funez, M.J. Ramos, J.L. Valverde, Liquid-phase hydroisomerization of n-octane over platinum-containing zeolite-based catalysts with and without binder, Ind. Eng. Chem. Res. 45 (2006) 8852–8859, https://doi.org/10.1021/ie060388s.

[47] A. Aranzabal, D. Iturbe, M. Romero-Saez, M.P. Gonzalez-Marcos, J.R. Gonzalez-Velasco, J.A. Gonzalez-Marcos, Optimization of process parameters on the extrusion of honeycomb shaped monolith of H-ZSM-5 zeolite, Chem. Eng. J. 162 (2010) 415–423, https://doi.org/10.1016/j.cej.2010.05.043.

[48] A. Torozova, P. Mäki-Arvela, N. Kumar, A. Aho, A. Smeds, M. Peurla, R. Sjöholm, I. Heinmaa, K.P. Volcho, N.F. Salakhutdinov, D.Y. Murzin, Isomerization of verbenol oxide to a diol with para-menthane structure exhibiting anti-parkinson activity, Reac. Kinet. Mech. Cat. 116 (2015) 299–314, https://doi.org/10.1007/s11144-015-0903-7.

[49] V.V. Zhivonitko, Z. Vajglová, P. Mäki-Arvela, N. Kumar, M. Peurla, D.Y. Murzin, Diffusion measurements of hydrocarbons in zeolites with pulse-field gradient nuclear magnetic resonance spectroscopy, Russ. J. Phys. Chem. 95 (2021) 547–557, https://doi.org/10.1134/S0036024421030250.

[50] K.Y. Lee, H.K. Lee, S.K. Ihm, Influence of catalyst binders on the acidity and catalytic performance of HZSM-5 zeolites for methanol-to-propylene (MTP) process: single and binary binder system, Top. Catal. 53 (2010) 247–253, https://doi.org/10.1007/s11244-009-9412-0.

[51] U.K. Singh, M.A. Vannice, Liquid-phase citral hydrogenation over SiO2-supported group VIII metals, J. Catal. 199 (2001) 73–84, https://doi.org/10.1006/jcat.2000.3157.

[52] F. Neatu, S. Coman, V.I. Parvulescu, G. Poncelet, D. De Vos, P. Jacobs, Heterogeneous catalytic transformation of citronellal to menthol in a single step on Ir-beta zeolite catalysts, Top. Catal. 52 (2009) 1292–1300, https://doi.org/10.1007/s11244-009-9270-9.

[53] V.K. Aggarwal, G.P. Vennall, P.N. Davey, C. Newman, Scandium trifluoromethanesulfonate, an efficient catalyst for the intermolecular carbonyl-ene reaction and the intramolecular cyclisation of citronellal, Tetrahedron Lett. 39 (1998) 1997–2000, https://doi.org/10.1016/S0040-4039(98)00115-4.

[54] D.Y. Murzin, T. Salmi, Catalytic Kinetics, Science and Engineering, Elsevier, Amsterdam, 2016.